ISBN: 978-3-95450-262-2 ISSN: 2673-5350 doi: 10.18429/JACoW-IBIC2025-MOPMO37

DEVELOPMENT OF CMOS BEAM LOSS MONITOR FOR KOREA-4GSR

Bokkyun Shin†,1, Garam Hahn[1], Dong Cheol Shin[1], Donghyun Song[1], Dotae Kim[1], Gyujin Kim[1], Seohyeon An[1], Siwon Jang[1], Changbum Kim[1], Jung Yun Huang[1], Woojin Song[2]
[1]Pohang Accelerator Laboratory, Pohang, Korea
[2]Postech, Pohang, Korea

Abstract

The beam loss monitor (BLM) is a diagnostic system designed to protect accelerator components from unexpected high-energy radiation. We have developed a cost-effective BLM system for the next-generation synchrotron light source, Korea-4GSR. The system utilizes plastic scintillators, optical fibers, and a CMOS camera to localize beam losses with a time resolution of 10 ms. Scintillators placed along the beam-line and emit blue light proportional to the energy deposited by loss particle. This light is transmitted through optical fibers, bundled into a 2D array, and imaged by a CMOS sensor operating at 100 Hz. The prototype, consisting of 10 BLM detectors, was calibrated using a 2.3 MBq Co-60 gamma-ray source. The end-to-end calibration results were consistent with analytical estimates. Energy deposition was simulated using Geant4, and the photon-to-ADC count conversion was characterized using a calibrated LED source. This presentation outlines the system design, calibration methodology, and performance evaluation of the prototype system.

INTRODUCTION

Beam loss monitoring is a critical component of accelerator operations, designed to detect unexpected beam losses, protect the machine, and diagnose the causes of losses. This system was designed based on the CMOS-based beam loss monitor developed for the SLS [1]. While slower in response compared to photomultiplier tube (PMT)-based systems, the CMOS-based BLM is significantly more cost-efficient, costing approximately one-tenth of a PMT-based system.

For the Korea 4GSR accelerator, the CMOS-based BLM will be used in conjunction with PMT-based systems. The CMOS-based BLM is primarily positioned for spatial monitoring, while the PMT-based BLM focuses on timing-critical applications.

BEAM LOSS MONITOR SYSTEM

The CMOS BLM system consists of detector and DAQ. The detector consists of a scintillator, a wavelength-shifting (WLS) fiber, and DAQ consists of a CMOS camera for optical signal readout. Figure 1 shows configuration of detector and DAQ.

The detector design evolved through two primary configurations. The first version employed a 15-meter-long scintillating fiber with a 1 mm core diameter, optimized for a large interaction volume. However, the long winding fiber introduced challenges in light collection efficiency and signal uniformity. In the second and current version, shown in Fig. 2, a flat scintillator plate (EJ-200, 100 mm × 100 mm × 10 mm) was adopted. The plate is coated with a highly reflective blue light material (EJ-510), which provides a reflectivity of 98 %. The WLS fiber was embedded in a groove along the perimeter of the plate.

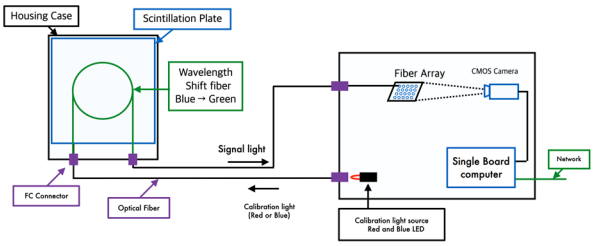

Figure 1: Configuration of the BLM System.

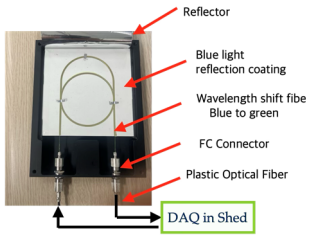

Figure 2: Configuration of Detector.

The scintillator emits photons within the 400–500 nm wavelength range, with a peak emission at 420 nm. These photons are absorbed by the wavelength-shifting (WLS) fiber, which has an absorption peak at 460 nm and re-emits green light centered at 520 nm. The re-emitted light is transmitted to the CMOS camera through a plastic optical fiber (POF; Mitsubishi GH-4001, 1 mm core diameter), which exhibits a measured attenuation of approximately 0.12 dB/m at 520 nm. The optical transmission path includes FC-type connectors to ensure modularity and ease of maintenance. The detector incorporates a dual-port configuration, enabling both signal acquisition and external light injection for calibration purposes.

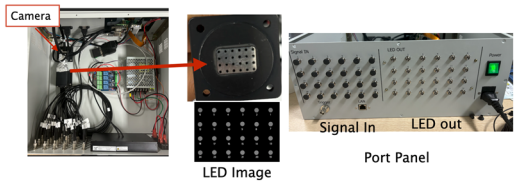

Figure 3: Configuration of the DAQ.

The data acquisition system shown in Fig. 3 employs a CMOS camera (acA720-520um, Basler) with a 10 mm lens (MCA-10, VS-Tech) to capture scintillation light. Standard

† bkshin@postech.ac.kr

ISBN: 978-3-95450-262-2 ISSN: 2673-5350 doi: 10.18429/JACoW-IBIC2025-MOPMO37

operation uses 100 Hz sampling, 10 ms exposure, 20 dB gain, and 12-bit ADC resolution.

The DAQ housing features a 6 × 4 grid array comprising 24 input ports, corresponding to the layout of the fiber bundle. It also includes 24 LED output ports used for calibration purposes (Fig. 3, bottom right). The input fibers are arranged in a 6 × 4 matrix with a 2 mm pitch and are positioned at a fixed working distance of 60 mm from the lens (Fig. 3, center). The spatial positions of the light spots from each fiber port are identified and calibrated using images acquired under LED illumination, ensuring accurate mapping of the signal integration regions on the CMOS sensor.

CALIBRATION

While both Cs-137 and Co-60 were considered for calibration, Co-60 was selected due to its approximately four times higher gamma yield, which results in a significantly stronger detector response. Table 1 summarizes the gamma-ray emission rates and corresponding ADC counts. The activities of both sources (in Bq) at the time of calibration, conducted in November 2022, were estimated based on their respective half-lives.

Calibration was performed using a 2.33 MBq Co-60 gamma-ray source, which emits photons at energies of 1.17 MeV and 1.33 MeV, yielding a total emission rate of approximately 4.67 million gamma photons per second. Although the CMOS camera typically operates with a 10 ms exposure time (corresponding to 100 Hz sampling), this configuration yielded an insufficient signal-to-noise (S/N) ratio for the low-level gamma source. Therefore, the exposure time was increased tenfold to 0.1 s to enhance signal acquisition. During calibration, the detector was operated at 20 dB gain and 12-bit ADC resolution. The ADC signal was measured as the difference between the average count with the source present and the average background count without the source.

Figure 4: Gamma source placed directly on the detector.

During signal measurements, the Co-60 source was placed directly on the center of the detector (Fig. 4). About 0.5 cm shifting from the center the response uncertainty is about 3 %. For background measurements, the source was enclosed in a 1 cm-thick lead shield and positioned approximately 1 meter away from the detector.

Table 1: Comparision of Sources

Source	Decay [MBq]	γ rate [Mγ/sec]	Energy [MeV]	S_{Signal}
Co-60	2.87	2.30	0.67	75.31
Cs-317	2.33	4.67	1.17, 1.33	311.4

ANALYSIS

To define the signal integration area on the CMOS sensor, LED illumination was employed. The LED light was injected through each optical fiber port, and the corresponding light spots were imaged by the CMOS camera to identify their spatial positions. Figure 5 shows the LED image acquired during this procedure. Based on the observed circular illumination patterns—approximately 40 pixels in diameter—an integration window of 44 × 44 pixels was selected for each port to ensure complete coverage of the illuminated region. The integrated signal (S, in ADC counts) was calculated by summing the pixel values within this fixed window across all recorded frames.

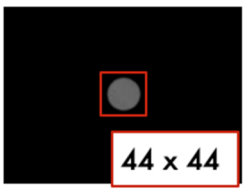

Figure 5: LED signal image.

The calibration signal was obtained by computing the difference between the average integrated signals measured with and without the radioactive source:

$$S_{signal} = \langle S_{source} \rangle - \langle S_{Background} \rangle.$$

In the calibration measurement, the average signal with the source present was approximately 2700 ADC counts, while the average background signal was around 2400 counts. Each measurement was averaged over 1,000 events to ensure statistical stability and reduce noise.

RESULT

Figure 6 presents the calibrated response (S_{signal}) for each detector ID measured at 2024 December. Calibration of ten detectors was performed in December 2024 and January 2025. Each detector was connected using 20-meter plastic optical fiber (POF) cables—both from the detector to the signal input port and from the LED to the same port. Detectors No. 1–5, which were manufactured earlier, did not include a blue light reflective coating, whereas Detectors No. 6–10 were fabricated with a blue-reflective coating. The application of the blue coating approximately doubled the photon collection efficiency, as observed in the measured signal levels. A relative end-to-end calibration factor was estimated for each detector as: $F_{cal\_i} = S_{signal\_i}/S_{signal.}$

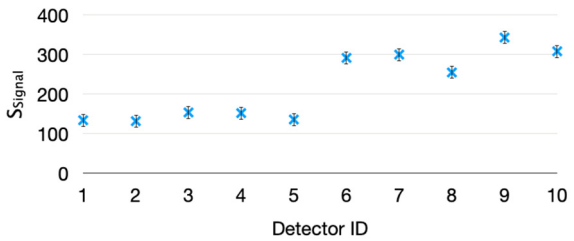

Figure 6: The S_{signal} result of 10 detectors using Co-60.

ISBN: 978-3-95450-262-2 ISSN: 2673-5350 doi: 10.18429/JACoW-IBIC2025-MOPMO37

The absolute signal difference between the measurements conducted in December 2023 and January 2024 was approximately 15 %. However, when normalized to the average signal, the relative variation was within 5 %, indicating good consistency in detector response over time.

The uncertainty in this relative calibration factor was estimated to be 5.8 %, which includes contributions from source positioning uncertainty (~3 %) and response reproducibility over time (~5 %). This level of uncertainty is considered acceptable for beam loss monitoring applications, where relative sensitivity among detectors is more critical than absolute calibration.

To validate the measured signal S_{signal}, a comparison was made between the simulation-based estimation and the expected signal calculated from the measured transmittance of the POF cable, connector losses, and the photon-to-ADC conversion efficiency of the CMOS camera. Equation (1) describes the overall signal calculation, representing the entire detection process from gamma-ray energy deposition to digitization by the CMOS sensor. Table 2 summarizes the values used for each component in the calculation.

$$S_{signal} = E_{loss} \times Y_{Scin} \times T_{WLS} \times C_{WLS} / 2 \text{ ports} \times T_{Con} \times T_{cable} \times T_{Con} \times T_{cable\_inner} \times R_{cam}. \quad (1)$$

Table 2: Component Parameters for Signal Prediction

Item	Result	Method
Energy Deposition (E_{dep})	88780 MeV/s	Sim.
Photon yield (Y_{scin})	10000 Photons/MeV	Sheet
WLS absorption rate (T_{WLS})	70 %	Sim.
Blue to green ratio (C_{WLS})	2.5 %	Meas.
Cable loss T_{cable} red	0.21 dB/m	Meas.
Cable loss T_{cable} blue ($1/(T_{cable}/L)$)	0.12 dB/m	Meas.
FC Connector loss ($1/T_{con}$)	3dB	Meas.
CMOS photon/ADC green (R_{cam})	762.7 photons /ADC	Meas.

An average energy deposition of 19.4 keV/1.3 MeV gamma photon and collection efficiency through the WLS fiber was estimated via Geant4 simulations [2]. Light emission of WLS, transmission losses in the POF cable and FC connectors, were measured using a calibrated LED light source and an optical power meter (PM101, Thorlabs). The POF loss was characterized for both 520 nm (green) and 650 nm (red) wavelengths, using the average values from 20 POF samples. FC connector loss was estimated from six different connector pairs. The blue-to-green conversion efficiency of the WLS fiber was also measured using 520 nm illumination.

The resulting estimated signal was $S_{signal} = 333 \pm 45$ ADC counts, which agrees well with the experimentally measured value, demonstrating the consistency between analytical prediction and end-to-end calibration.

CONCLUSION

A cost-effective CMOS-based beam loss monitoring (BLM) system has been developed and calibrated for use in the Korea-4GSR synchrotron radiation facility. The system demonstrated adequate spatial resolution and sensitivity using a flat scintillator with reflective coating, WLS fiber, POF cables, and a CMOS camera-based DAQ system operating at 100 Hz.

Calibration with a Co-60 gamma-ray source validated that relative response calibration among detectors is sufficient for beam loss localization and monitoring. Absolute calibration was shown to be unnecessary, as the system is primarily used for comparative signal analysis. The observed detector-to-detector response variation was within 5.8 %, including source placement and optical variations.

In the final system configuration, beam loss detectors will be deployed as fixed Detector–Cable pairs, and end-to-end calibration will be performed on each pair to account for component-dependent variations. These results confirm the system's readiness for deployment in large-scale accelerators, offering an economical and effective alternative to conventional PMT-based systems.

ACKNOWLEDGEMENTS

This research was supported in part by the Korean Government MSIT (Multipurpose Synchrotron Radiation Construction Project) (RS-2022-00155836)

REFERENCES

[1] C. Ozkan Loch, R. Ischebeck, and A. M. M. Stampfli, "CMOS Based Beam Loss Monitor at the SLS", in *Proc. IBIC'21*, Pohang, Korea, Sep. 2021, pp. 186-188. doi:10.18429/JACoW-IBIC2021-TUOB02

[2] S. Agostinelli et al., "GEANT4—a simulation toolkit", *Nucl. Instrum. Methods Phys. Res. A*, vol. 506, no. 3, pp. 250–303, 2003.